

## Application of ground-penetrating radar and high-density electrical sounding for the study of seasonally frozen ground

Takayuki NAKANO and Hideo SAKAI

Graduate School of Science and Engineering, University of Toyama, 3190, Gofuku, Toyama, 930-8555 Japan

(Received September 28, 2006; Revised manuscript accepted November 25, 2007)

### Abstract

Ground-penetrating radar (GPR) and high-density electrical sounding surveys were conducted on a seasonally frozen ground at the Kitami Institute of Technology, northern Japan. The GPR survey detected the frozen ground as a weak echo zone in two and/or three dimensions. The high-density electrical sounding surveys showed that the electrode arrangement of the Wenner array effectively revealed the frozen layer as a resistive zone. The frost depth estimated from both surveys, especially the GPR profile, corresponded well to measurement done by a frost depth meter (frost tube). The results of this study show the applicability of non-destructive surveys in geophysical exploration on seasonally frozen ground. GPR surveys could be especially effective in conducting repeated investigation on large areas of seasonally frozen ground.

### 1. Introduction

Formation of frozen ground causes frost heave. In cold regions, this frost heave may disrupt human lives due to the deterioration of pavements and/or buildings. The mechanism of frozen ground development has been studied to date. In general, a frost depth meter (frost tube) and thermometer are used to investigate the distribution and thickness of the seasonally frozen ground. These apparatus are inserted vertically into the target spot; therefore, the depth information is limited to that spot. In recent years, a number of geophysical explorations have been conducted to study frozen ground (*e.g.*, Hauck, 2005; Yoshikawa *et al.*, 2006), and further development of these techniques is anticipated in the future. Resistivity prospecting is one of the major methods used to estimate frost depth or frozen areas (*e.g.*, Ishikawa and Hirakawa, 2000; Hauck *et al.*, 2003). However, these studies were conducted in permafrost areas, and few studies have been conducted on seasonally frozen ground (*e.g.*, Takami *et al.*, 2002). In this study, we applied a ground penetrating radar (GPR) survey and high-density electrical sounding (resistivity sounding) to estimate the frost depth of seasonally frozen ground at experimental sites in the Kitami Institute of Technology, northern Japan.

### 2. Outline of experiments

GPR survey is a visualization technique used to obtain an image of subsurface structure by the reflection, permeation, and refraction of radio waves at subsurface electromagnetic boundaries. It has also been used to study the subsurface permafrost distribution (*e.g.*, Hinkel *et al.*, 2001). On the other hand, high-density electrical sounding represents resistivity prospecting using several electrodes arranged in a straight line. We examined the efficiency of each method in detecting seasonally frozen ground by comparing the results obtained from them.

We surveyed two sites (A and B) at the Kitami Institute of Technology in February 2000. The apparatus used for the GPR survey was a pulse EKKO 1000 (Sensors & Software Inc., Canada). The two antennas (receiver and transmitter) were fixed to maintain an antenna separation of 0.25 m for 450-MHz and 0.17 m for 900-MHz. These antennas were moved systematically along the survey line with a spacing of 0.1 m. The profile analysis was performed using dewow filter (signal saturation correction, which removes an unwanted low frequency) and filter of vertical and horizontal direction.

The apparatus used for the high-density electrical sounding was E60B (GeoPen, China). The Wenner electrode configuration (Telford *et al.*, 1990) was adopted because it provides an excellent estimation of a

horizontal structure. We performed two-dimensional model analysis by applying inversion (least-squares method) to the primary model using the software E-Tomo (Dia Consultants Co., Japan).

### 2.1 Survey at Site A

Site A is a rectangular area (5 m × 2 m) composed of volcanic ash clay from the ground surface to a depth of approximately 1 m with basal ash lying below this depth. Frost tubes, thermometers and a device to observe the amounts of frost heaving are also installed at this site (Fig. 1). The frost tube consists of inner and outer tubes. The inner tube, which is made of acrylic resin and filled with 1% methylene blue aqua, has an outer caliber of 25 mm, inner caliber of 20 mm, and length of 1.5 m. The outer tube, made of vinyl chloride, has outer and inner calibers of 38 and 30 mm, respectively. The frost depth was observed daily and the ground temperature was measured every two hours from November to March. The temperatures were measured at vertical spacing of every 5 cm (0–1 m in depth) and every 10 cm (1–1.2 m in depth). In addition, the snow accumulated on the surface of the investigated area was removed during winter.

We set 21 survey lines at Site A. Line 1 (5.1 m in length, survey point spacing of 0.1 m) was set parallel to the longitudinal direction of this area, and both surveys were conducted along this line. Lines 2–21 (1.5 m in length, survey point spacing of 0.1 m and survey line spacing of 0.2 m) were set up perpendicular to Line 1, and only the GPR survey was performed along these lines (Fig. 2).

In the GPR survey, an antenna with a center frequency of 450-MHz was primarily used, while surveys using a 900-MHz antenna were also conducted on Lines 1, 2, 7, 16, and 18. Radio waves radiate conically from the antenna into the ground. If the average relative dielectric constant of frozen ground is assumed to be 6 (Society of Exploration Geophysicists, 1998), the effective distance is approximately 0.2 m at the depth of 0.5 m from a survey point in the direction perpendicular to the scanning antenna direction using the 450-MHz antenna. Thus, the surveys cover all the target area with these survey points and lines spacing. The spatial resolutions of the radio waves in the ground are approximately 0.1 m at 450-MHz and 0.06 m at 900-MHz, as estimated from the propagation velocity of the radio waves (0.10–0.12 m ns<sup>-1</sup> described in subsection 2.3). Thus, these resolutions are sufficient to estimate the distribution of the frozen ground.

High-density electrical sounding was conducted along Line 1. The electrode spacing and length of survey line were set to 0.2 and 5.2 m, respectively. Since pitching electrodes into the frozen ground was difficult, it was expected that the ground resistance would increase.



Fig. 1. Photograph of Site A.

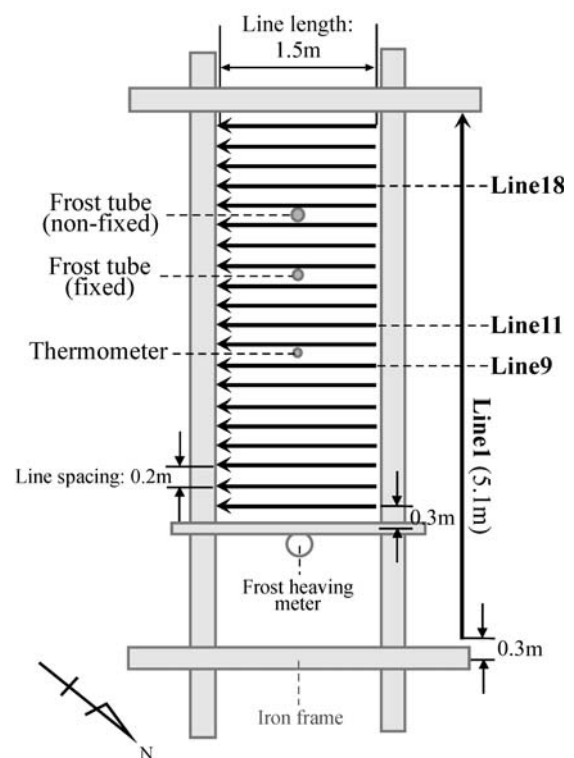


Fig. 2. Arrangement of survey lines at Site A. Thick arrows are the survey lines.

### 2.2 Survey at Site B

Site B is an artificial pit area with a depth of 1.3 m; it is surrounded by a concrete wall and filled with testing soil (Fig. 3). The internal testing soil is composed of volcanic ash clay (0–0.9 m in depth) and gravel (0.9–1.3 m in depth) (Fig. 4). A water pipe is installed at the bottom of the pit, where the gravel is filled to control a uniform groundwater level. As shown in Fig. 4, we set 14 survey lines (2.7 m in length, survey point spacing of 0.1 m, and survey line spacing of 0.2 m) for the GPR survey. A 450-MHz antenna was used at this site.

### 2.3 Estimation of propagation velocity of radio waves

In the GPR survey, we did not conduct the com-

mon midpoint (CMP) survey (Telford *et al.*, 1990), which estimates the propagation velocity of radio waves in the ground. Consequently, at each site, the propagation velocity is estimated as follows:

[1] Site A: The propagation velocity of the radio waves is calculated using the following equation:

$$V = c / \sqrt{\epsilon_r},$$

where  $c$  is  $3.0 \times 10^8 \text{ m s}^{-1}$  and  $\epsilon_r$  is the relative dielectric constant of the medium. When the relative dielectric constant of the frozen ground is 4–8 (Society of Exploration Geophysicists, 1998), the propagation velocities become  $0.11\text{--}0.15 \text{ m ns}^{-1}$ . Because the relative dielectric constant of frozen ground is affected by the amount of ice and unfrozen water in the soil, the velocities at this site could not be ascertained. Therefore, we used the central value of  $0.12 \text{ m ns}^{-1}$  ( $\epsilon_r = 6$ ) to calculate the approximate depth.

[2] Site B: The strongest reflection appeared at 25 ns in travel time, which was the reflection from the basal concrete wall at the depth of 1.3 m. Subsequently, the velocity was calculated to be  $0.10 \text{ m ns}^{-1}$ , which we considered to be the average propagation velocity in this pit.

### 3. Results

#### 3.1 Site A

Table 1 shows the daily mean temperature on the surveyed day. Figure 5 shows the water content measured from a boring core sample at Site A. The frost depth measured using the frost tube was 76.1 cm. As the amount of frost heaving was 6.2 cm, the thickness of the frozen ground was approximately 82 cm.

Table 1. The daily mean temperature on the surveyed day [Feb. 28, 2000] at Site A.

Depth (cm)	Temperature (°C)
Air temperature	−9.2
surface	−8.1
0	−8.5
5	−8.3
10	−8.1
15	−7.6
20	−6.9
25	−6.1
30	−5.6
35	−5.5
40	−4.8
45	−4.4
50	−3.9
55	−3.3
60	−2.8
65	−2.1
70	−1.7
75	−1.8
80	−1.1
85	−0.7
90	−0.2
95	0.1
100	0.5
110	1.2
120	1.9



Fig. 3. Photograph of Site B.

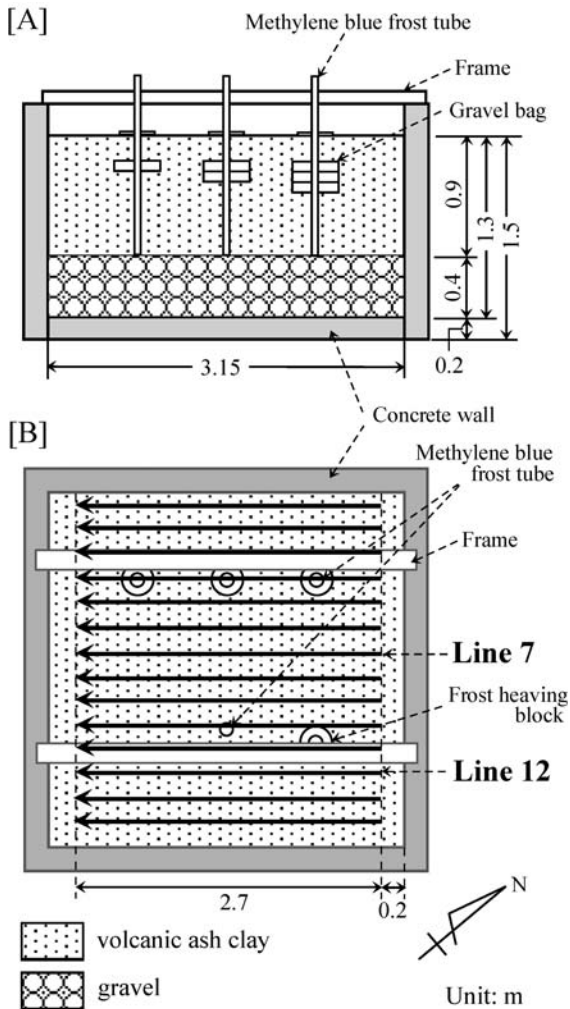


Fig. 4. Structure of the artificial pit at Site B. [A] A vertical cross section. [B] A horizontal layout from the top. Thick arrows are the survey lines.

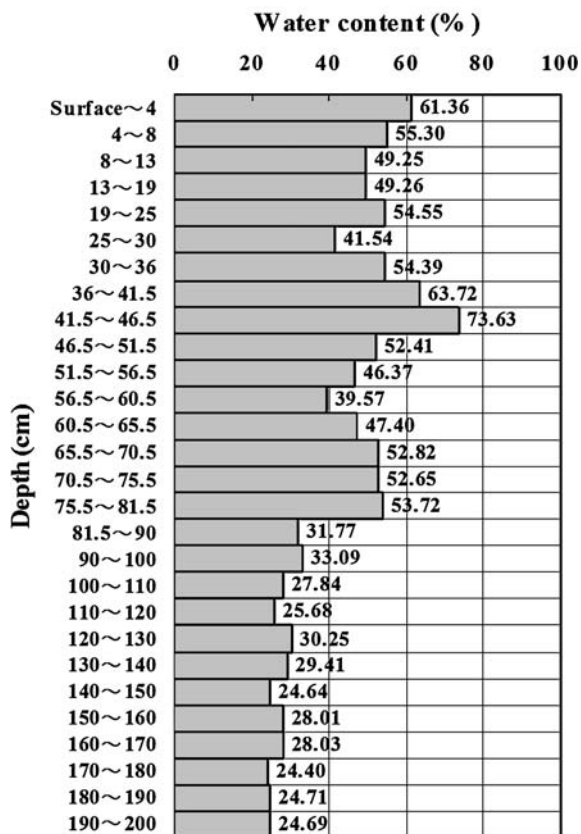


Fig. 5. The water content measured from a boring core at Site A.

Figure 6 shows the GPR profile along Line 1 obtained using the center frequency of the 900- and 450-MHz GPR antennas. The color tones of the profile represent the strength of the echo; the darker color indicates a stronger echo. The differing resolutions at the two frequencies resulted in slightly different distributions of echo strength at the different depths. However, the overall echo patterns were almost similar to each other. A weak echo zone above the depth of about 0.6–0.8 m corresponds to the frozen ground, as can be seen on comparison with the abovementioned measurements. Thus, a strong echo zone below this depth represents unfrozen ground.

Figure 7 shows the survey profiles of three typical survey lines (Lines 9, 11, and 18) obtained using the center frequency of the 450-MHz GPR antennas. The weak echo zone between the surface and the depth of 1 m is recognized to be frozen ground (as in the case of Line 1), and the freezing front is found to be uneven. This indicates that the depth of the freezing front or the thickness of the frozen ground varies in each survey line. A lengthwise echo in the deeper part around the centers of Lines 9 and 11 may be a reflection from the buried thermometer.

Thus, the results of the GPR profiles correspond well with the actual frost depth, and the three-dimensional figure (Fig. 8) composited from the profiles along Lines 2–21 shows similar result. This

shows the unevenness of the freezing front in a small area. In addition, the depth of the freezing front is deeper around the center of the survey area. It appears that the ground does not freeze easily near the edge of the survey area, due to the warming effects of the snow cover on the neighboring areas.

At this site, a high-density electrical resistivity survey was conducted along Line 1 using the Wenner array (Fig. 9). In Fig. 9, the upper and lower figures show a typical figure of electrode arrangement and the theoretical distribution of the measurement points, respectively. Figure 10 shows the interpreted result. There exists a resistive layer above the depth of approximately 1 m, except for the subsurface. Considering the results of Table 1, it is presumed that the resistive layer at the depth of 1 m corresponds to the frozen ground.

### 3.2 Site B

In this site, the frost depth measured using the frost tube was 57.5 cm, and the amount of frost heaving was 12.9 cm, indicating that the thickness of the frozen ground was about 70 cm. The GPR profiles of Lines 7 and 12 measured using a 450-MHz antenna are shown in Fig. 11. A strong echo at the travel time (left axis) of 25 ns was considered to be from the concrete bottom of the pit at the depth of 1.3 m, while a weak echo zone was observed from the surface to a depth of approximately 0.6 m. We considered the weak echo zone to be the frozen ground, although the freezing depth estimated from the GPR survey differed slightly from that measured using the frost tube. We inferred that this difference was caused by the application of the average propagation velocity of the radio wave to the profile analysis. The irregular echo around 0.5–1 m in the horizontal direction on Line 12 could be attributed to the influence of the frost heaving block (an observation device).

There is a strong echo from the freezing front to a depth of approximately 0.9 m, corresponding to the unfrozen volcanic ash clay layer. The lower weak echo zone corresponds to the gravel layer. This indicates that the relative dielectric constant of the gravel layer is higher than that of the volcanic ash clay layer. In general, the relative dielectric constant of volcanic ash clay and gravel are in the range of 2 to 6 when they are dry (Society of Exploration Geophysicists, 1998; Kobayashi and Sato, 2004). However, the echo pattern of the GPR survey indicates obvious differences in their dielectric properties. This was interpreted as an indication that the gravel layer contained many air gaps filled with unfrozen water and that it had a higher relative dielectric constant.

Figure 12 shows the three-dimensional figures composited from the profiles along all survey lines; in this figure, [A] shows the overview and [B] and [C] show the partial cross sections of [A] at arbitrary

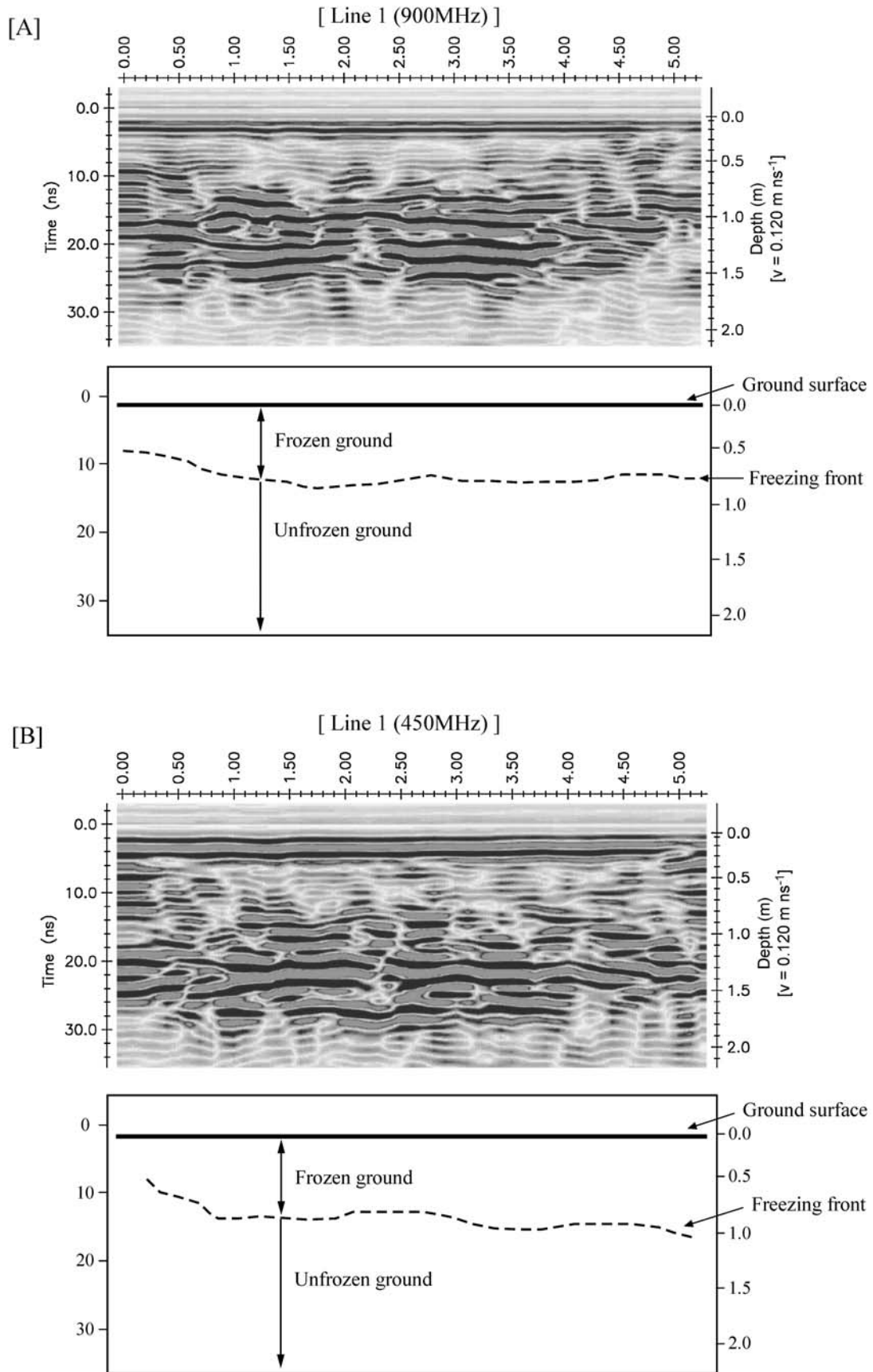


Fig. 6. GPR profiles (each upper figure) and the interpreted results (each lower figure) along Line 1 at Site A. The left axis shows the travel time, and the right axis shows the estimated depth. [A] The center frequency of 900-MHz. [B] The center frequency of 450-MHz.

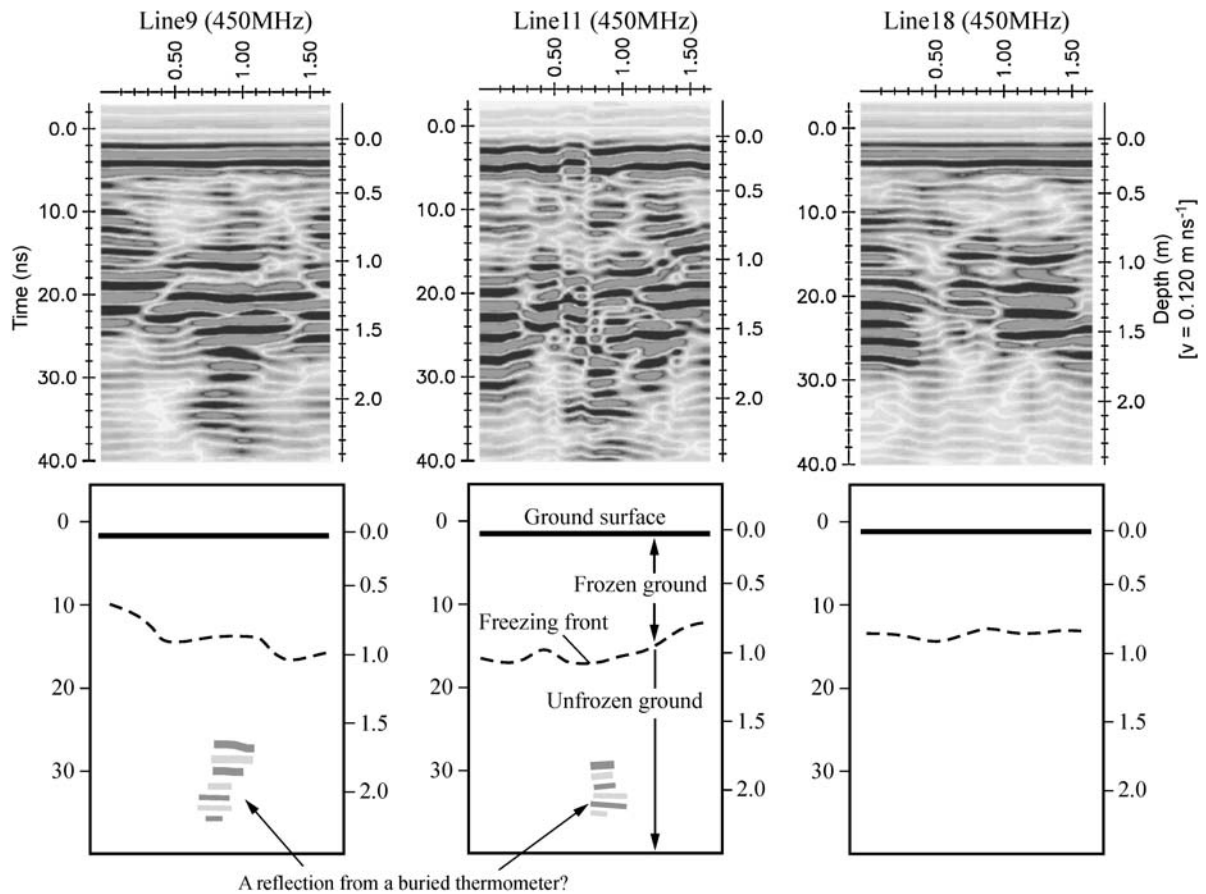


Fig. 7. GPR profiles (upper figures) and interpreted results (lower figures) along Line 9, 11, and 18 at Site A using the center frequency of 450-MHz GPR antennas.

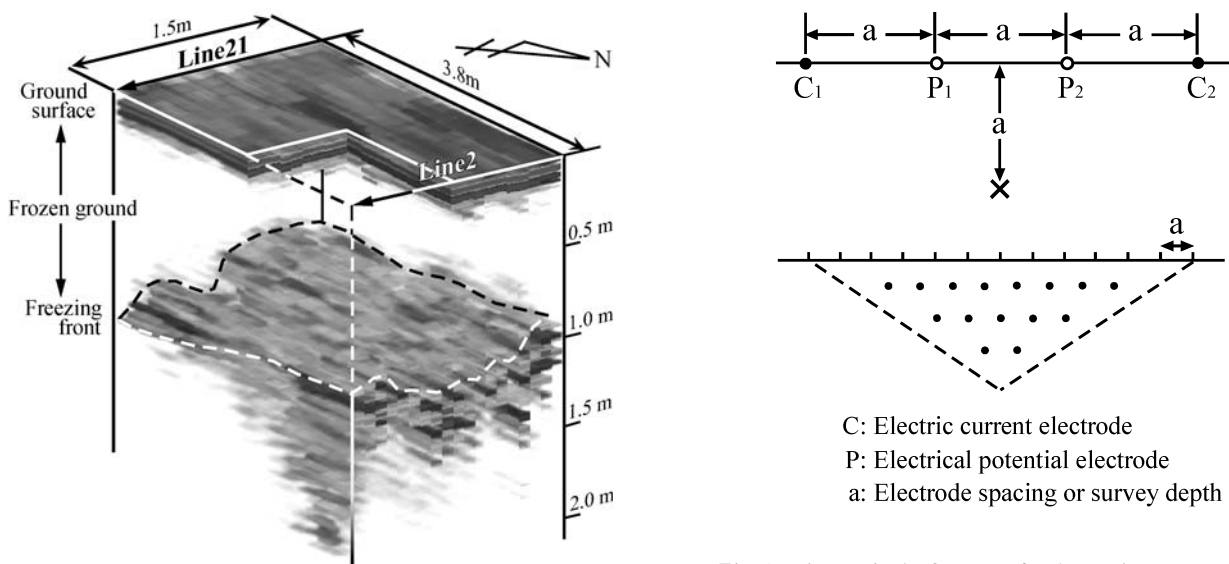


Fig. 8. The three-dimensional figure composed from the profiles along Lines 2-21 at Site A.

Fig. 9. A typical figure of electrode arrangement (upper figure) and the theoretical distribution of the measured points (lower figure) at the Wenner array. The C and P show an electric current and electric potential electrodes, respectively. The “a” show electrode spacing or survey depth.

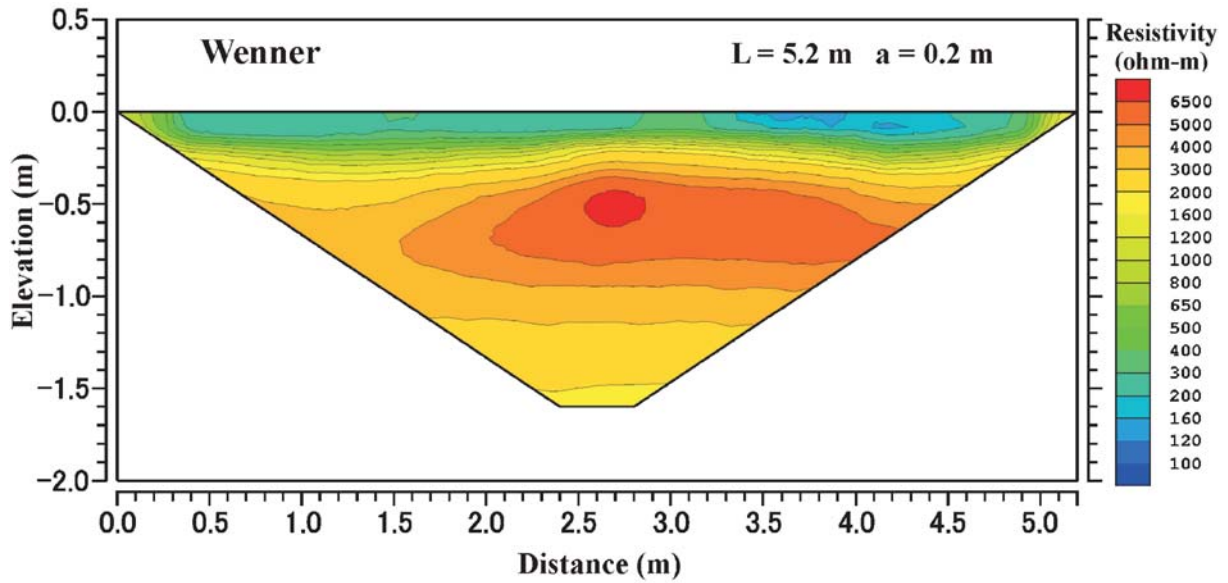


Fig. 10. Interpreted result from the high-density electrical survey by the Wenner array along Line 1 at Site A. The L is survey line length. The “a” is electrode spacing.

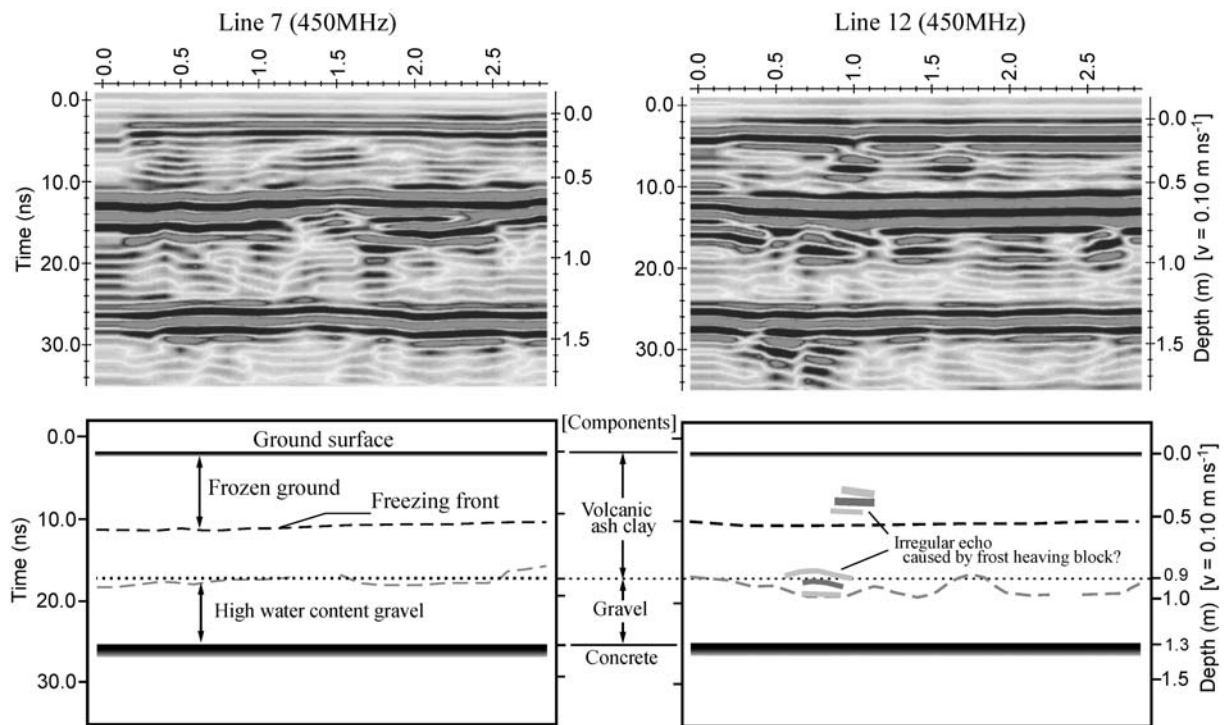


Fig. 11. GPR profiles (upper figures) and the interpreted results (lower figures) along Line 7 and 12 at Site B. The center frequency of the antenna is 450-MHz.

planes along Line 7. This shows that the internal structure of each section is very similar.

#### 4. Discussions

The frozen ground was detected as a weak echo zone in the GPR profile. This weak echo zone may have appeared because the relative dielectric constant

was homogenized due to the growth of the frozen ground and an increase in the amount of ice.

In the case of Site A, the freezing front detected on the GPR profiles is uneven in a small area. In other words, the frost depth measured using the frost tube does not represent the typical frost depth around the investigation area, unless the measurement is performed at a large number of well-distributed points.

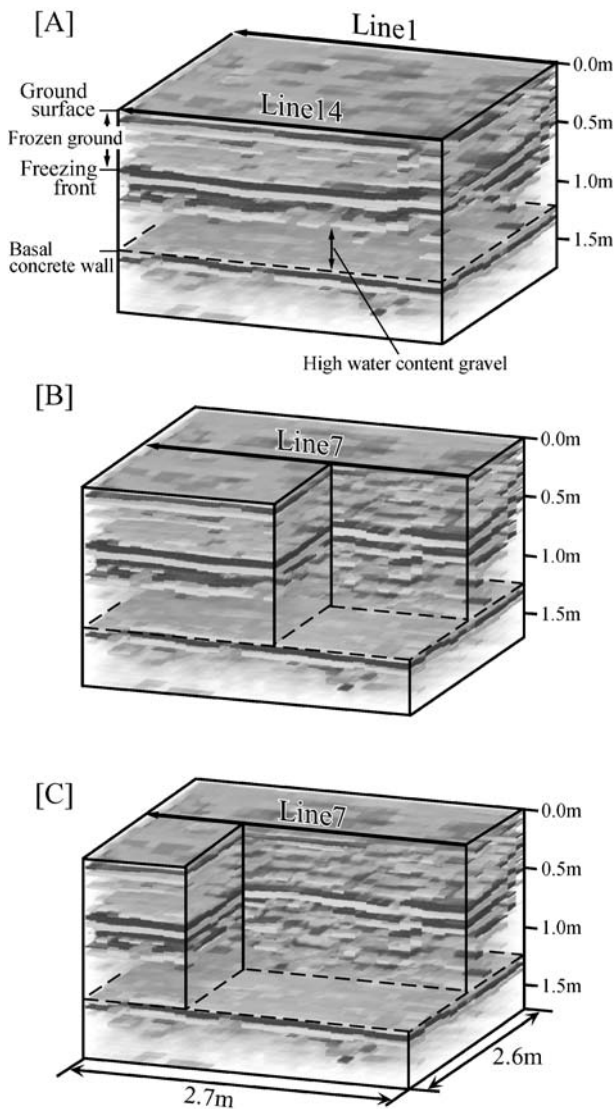


Fig. 12. Three-dimensional figures composited from the profiles along all survey lines at Site B. [A] shows the overview and [B] and [C] show the partial cross sections of [A] at arbitrary planes along Line 7.

The interpreted result of the high-density electrical resistivity survey conducted using the Wenner array shows the frozen ground as a resistive layer. The subsurface low resistivity layer shown in Fig. 10 may have been caused by the decrease in the electric potential due to the water from melting snow. As the survey day was sunny, a small amount of snow on the surface around the electrodes may have thawed due to sunshine, although the temperature was at subzero level.

It has been shown that the GPR survey and high-density electrical sounding can detect seasonally frozen ground. The GPR survey offers higher mobility and repeatability, and can detect the planar structure of the freezing front clearly. Further, although the electrical resistivity survey offers the advantage of deeper skin depth compared to the GPR survey, the skin depth of the latter is sufficient to investigate the

seasonally frozen ground. Moreover, in the resistivity survey, there exists the possibility of increase in the ground resistance and decrease in the electric potential due to the water from melting snow. Therefore, we consider that the GPR survey is more suitable for investigating the distribution of seasonally frozen ground over a large area.

At Site B, the freezing front presumed from the profile is flat, in contrast to Site A. The GPR echo pattern of all survey lines are similar, which may be caused by the artificially controlled water supply in the pit and the uniform rate of ground freezing.

## 5. Conclusions

The efficiency of non-destructive investigations on frozen ground was studied through experimental surveys. A GPR survey and a high-density electrical sounding method revealed the following results:

- (1) In the GPR study, seasonally frozen ground was detected as a weak echo zone. We considered that the radio waves were not strongly reflected because an increase in the amount of ice in the seasonally frozen ground had homogenized the relative dielectric constant.
- (2) From the GPR profiles, the freezing front could be displayed as a planar structure. At Site A, the detected freezing front was uneven. The thickness of the seasonally frozen ground may change depending on the location, even in a small area under natural conditions. Therefore, expansive investigation and three-dimensional analysis using a GPR survey are important and effective methods for the study of seasonally frozen ground distribution.
- (3) In an artificial pit (Site B), where the soil was packed into the pit and the water supply was controlled, the freezing front was ascertained to be almost flat based on the GPR profiles.
- (4) The electrical resistivity survey using the Wenner array detected the seasonally frozen ground as a resistive layer. The area corresponded well to the seasonally frozen ground area measured by the frost tube.

The GPR survey and high-density electrical sounding are both effective methods for the study of seasonally frozen ground. A comparison of the two methods reveals that the GPR survey offers higher mobility and repeatability and can detect the planar structure of the freezing front more clearly. Further, in the resistivity survey, there exists a possibility that the ground resistance may increase and the electric potential may decrease due to the water from melting snow. Therefore, the GPR survey is more suitable for investigating the distribution of seasonally frozen ground over a large area, and it will contribute to the study of frozen ground formation by continuous observation of the same area.

## Acknowledgments

The authors would like to thank Professor Teruyuki Suzuki and the staff at the Kitami Institute of Technology for their support in this study. We also provide grateful thanks to Mr. Yasushi Tanaka at the resistivity survey. This manuscript was improved by the insightful review of Dr. Nozomu Naito and an anonymous reviewer.

## References

- Hauck, C. (2005): Detecting and monitoring frozen ground and unfrozen water content using electric and electromagnetic techniques. Proceedings of the 6th Conference on Electromagnetic Wave Interaction with Water and Moisture Substances, ISEMA 2005, Weimar, Germany, 519–526.
- Hauck, C., Vonder mühl, D. and Maurer, H. (2003): Using DC resistivity tomography to detect and characterize mountain permafrost. *Geophysical Prospecting*, **51**, 273–284.
- Hinkel, K.M., Doolittle, J.A., Bockheim, J.G., Nelson, F.H., Paetzold, R., Kimble, J.M. and Travis, R. (2001): Detection of subsurface permafrost feature with ground-penetrating radar, Barrow, Alaska. *Permafrost and Periglacial Processes*, **12** (2), 179–190.
- Ishikawa, M. and Hirakawa, K. (2000): Mountain permafrost distribution based on BTS measurements and DC resistivity soundings in the Daisetsu Mountains, Hokkaido, Japan. *Permafrost and Periglacial Processes*, **11** (2), 109–123.
- Kobayashi, T. and Sato, M. (2004): Optimization of GPR array antenna separation for landmine detection with FTDT simulation (in Japanese). *Bulletin of Information Synergy Center, Tohoku Univ.*, **37** (4), 3–10.
- Society of Exploration Geophysicists (1998): *Exploration Geophysicists Handbook* (in Japanese). Society of Exploration Geophysicists, Tokyo, 1336pp.
- Takami, M., Tsuchiya, F., Goto, N., Muto, A. and Yoshida, T. (2002): Electrical prospecting for seasonal frozen ground — Study of freeze-thaw process and analysis of frost depth (in Japanese). *BUTSURI TANSA (Physical Exploration)*, **55** (6), 523–536.
- Telford, W.M., Geldart, L.P. and Sheriff, R.E. (1990): *Applied Geophysics Second Edition*. Cambridge University Press, Cambridge, 770pp.
- Yoshikawa, K., Leuschen, C., Ikeda, A., Harada, K., Gogineni, P., Hoekstra, P., Hinzman, L., Sawada, Y. and Matsuoka, N. (2006): Comparison of geophysical investigations for detection of massive ground ice (pingo ice). *Journal of Geophysical Research*, **111**, E06S19, doi: 10. 1029.